A Carbon Nanotube Spiking Cortical Neuron with Tunable Refractory Period and Spiking Duration

Jonathan Joshi, Alice C. Parker, and Chih-Chieh Hsu
Ming Hsieh Department of Electrical Engineering
University of Southern California

***Abstract*— This paper describes an analog tunable carbon nanotube axon hillock that exhibits spiking with control over spiking frequency and spiking duration. Experiments with the axon hillock circuit embedded in a neuron circuit demonstrate spiking patterns similar to a biological fast-spiking neuron. The circuit design is biomimetic and changes in control voltages lead to changes in key spike parameters such as spike refractory period and spiking duration. The effect of change in output spiking frequency is tested with synapses that temporally summate, and their effect on neural firing is observed. The experiments are demonstrated with SPICE simulations using carbon nanotube transistor simulation models.**

I. Introduction

Most biological neurons fire by emitting several closely-spaced spikes or a burst of spikes when input stimulation is sufficient to cause spiking. The biological mechanism behind a neural spike is well understood [1]. Bursts of spikes or higher-frequency spike trains are more likely to result in relaying sensory inputs to the cortex than lower-frequency trains [2]. Neurons in the visual cortex respond with varying frequency when there is a detection of an edge at a particular orientation [3], depending on the contrast of the edge.

Spiking neurons can be classified into many types [4]. A recent publication [5] describes neurons in the somatosensory cortex that are classified as either Regular Spiking (RS) pyramidal or Fast Spiking (FS) interneurons. RS neurons have a higher spiking rate from the onset of spiking and settle down to a base frequency whereas FS cells have a high frequency from onset itself, and cease spiking completely when the cell membrane potential drops below a critical threshold.

This paper describes a carbon nanotube circuit design of a tunable spiking axon hillock, as a part of a typical cortical neuron that behaves much like a biological fast-spiking neuron. The circuit design is biomimetic and sections of the circuit can be directly linked to fundamental biological spiking mechanisms. The novel design has voltage controls in different sections of the circuit that tune the design, changing key spiking parameters such as refractory period (spiking frequency) and the total duration of spiking. We demonstrate the effect of change in frequency by impinging the output action potentials of the neuron onto a similar neuron with synapses that temporally summate. The simulation results demonstrate that a higher spiking frequency is necessary to raise the dendritic potential in the post-synaptic neuron enough so that the second neuron fires. This design is believed to be novel with respect to its embedded feedback controls over total spiking duration, and its completely analog implementation, as well as the circuit implementation using carbon nanotube transistor models. Another version of the circuit to be reported on later exhibits tonic spiking and membrane voltage-dependent spiking frequency, behaving much as its biological regular-spiking neural counterpart.

Support for this research has been provided by the Viterbi School of Engineering and the WiSE program at the University of Southern California, and this material is based upon work supported by the National Science Foundation under Grant No. 0726815. Any opinions, findings, and conclusions or recommendations expressed in this material are those of the author(s) and do not necessarily reflect the views of the National Science Foundation.

II. Background

Liu and Frenzel's spike train neuron is sn early mixed-signal electronic neural model [6]. Hynna and Boahen [7] describe a silicon thalamic relay neuron that exhibits tonic firing, then bursts with sufficient simulation. This neuron uses a spiking circuit [8] that depends on an off-chip reset signal from a digital circuit to regenerate a spike. Farquhar and Hasler [9] describe a biomimetic axon hillock circuit, and demonstrate changes in spiking frequency when different amplitudes of current are injected into the circuit. An electronic neuron design with both inhibition and excitation models a bursting oscillator with a depressed synapse constructed of a current mirror and amplifier, with the circuit modulating the output current of the synapse [10] without control over frequency or spiking duration. These oscillators are found in central pattern generators in neural circuits. Work done by Indiveri [11] presents a firing circuit similar to our axon hillock circuit in terms of the refractory period control but lacks control over variations in total spiking duration.

Carbon nanotubes (CNTs) can behave as metallic wires as well as FETs. CNTs are a few nm in diameter. Current flow is largely ballistic (comparable to the flow of electrons in free space), capacitances are in attofarads, and rise and fall times in picoseconds. Channel resistance is primarily due to the quantum resistance at the junction between the nanotubes and metallic connections. Current flow between drain and source is less easily controlled than with CMOS circuits. Appropriate interfaces could be used to convert to/from biological signal levels and delays. Nanotubes induce minimum immune system reactions in living tissue [12].

Single-walled carbon nanotubes avoid most of the scaling limits of silicon [13]. Paul *et al*. [14] demonstrated that carbon nanotube field-effect transistors (CNFETs) are less sensitive to the geometry-related process variations than silicon MOSFETs. Carbon nanotubes have the potential to be configured into 3-D arrangements, a capability we believe will become critical when implementing larger portions of the cortex due to the massive connectivity. Carbon nanotube circuits have the potential to be reconfigured in real time, a capability we feel is essential for learning. A technique has been proposed recently to design CNT circuits immune to misalignment and mispositioning that can guarantee the correct function being implemented [15]. Liu, Han and Zhou have demonstrated directional growth of high-density carbon nanotubes on a- and r-plane sapphire substrates [16]. They have developed a novel nanotube-on-insulator (NOI) approach, and a way to transfer these nanotube arrays to flexible substrates.

A CNFET device model with circuit-compatible structure including typical device non-idealities is used in our simulations. [17]. The strength of our model and similar models is the correspondence between individual circuit elements and specific physiological mechanisms in the biological neuron that allow us to vary axon hillock behavior easily with control inputs. This, and our choice of carbon nanotube technology, differentiates this work. However, we are investigating alternatives; a CMOS chip with basic neural circuits is being fabricated, and other nanotechnologies are under investigation.

III. The Carbon Nanotube Neuron Circuit

Our basic cortical neuron [18] consists of four types of submodules: the basic excitatory synapses ([19]), the simplified dendritic arbor [20] and the axon hillock. Circuit models for the dendrites are not provided here. We have used four synapses [20] and tuned the threshold of the axon hillock so that it spikes when all four synapses exhibit a typical EPSP.

The synapse implemented in the neuron is a biomimetic depolarizing excitatory synapse circuit, with correspondence between biological mechanisms and circuit structures. This circuit models cell potentials and neurotransmitter concentrations with voltages, with a correspondence between circuit elements and biological mechanisms.

The adder circuit in the simplified dendritic arbor [21] has been shown previously [20]. The dendritic arbor portion used for testing was published earlier [20].

There are four excitatory synapses in the arbor, each on a separate dendritic branch. Previous work [19] has shown that the synapses used in our neuron have the capability of temporal summation.

A. Biomimetic Axon Hillock Circuit

In a biological neuron, the axon hillock has the highest density of sodium channels, resulting in the lowest threshold (-55 mV) compared to elsewhere in the neuron to initiate an action potential. As shown in Figure 1, if the summation of post-synaptic potentials (PSPs) connected to the gate of transistor X2 reaches a threshold value, the *Gated Ion Channel section* raises its potential at point A indicating the opening of a voltage-gated ion channel. The raised potential at A is inverted to turn on PMOS X7 and the axon hillock circuit will initiate spiking. To mimic a fast-rising phase (due to the rapid increase of the sodium channel conductance) and a slower falling phase (due to the slower increase of the potassium channel conductances) of an action potential, we adjusted the pull-up and pull-down strengths of transistors X7, X8 and X9. Inverters 1 and 2 in the *Potassium Delay* were tuned to model the time courses (time constants) in the dynamic mechanisms of the voltage gated ion channels. The *Sodium Ion Delay Section* controls the delay for which the sodium channel conductance remains deactivated by turning off transistor X8. The voltage across the gate of transistor X15 (*refractory period control*) controls the spiking refractory period and hence spiking frequency. The voltage across the gate of transistor X4 (*Spiking Duration Control*) in the *Gated Ion Channel Section* controls how fast the voltage at point A will decay and hence controls the overall duration of spiking.

In a typical biological neuron, potentials range from around -75 mV to +40 mV with action potentials peaking around +40 mV. Since the carbon nanotube neuron is designed to operate with Vdd around 0.9 V as the peak action potential voltage, and with 0.0 V (Ground) as the resting potential, the post-synaptic potentials were scaled accordingly, with 0.0 V circuit potential corresponding to -75 mV biological potential and 0.9 V circuit potential corresponding to 40 mV biological potential. We scaled the delays with about 1 ms in the biological neuron scaling to about 10 ps in the nanotube neuron [22]. The postsynaptic potential appearing at the dendritic trunk is approximately 14% of the action potential and the duration is about 6 times as long as the action potential, similar to biological EPSPs described in the literature.

IV. Experiments With The Cortical Neuron

The neuron was tested with action potentials input to each synapse, and the output of the neuron measured. As shown in Figure2 the input APs 1 and 2 (green trace, superimposed) cause the dendritic potential (red trace) to rise and cause the axon hillock to produce spikes (purple and blue traces). As we observe in Figure 2, by varying the *Spiking Duration Control* voltage, the spiking duration in the upper trace (purple trace) can be adjusted longer than the spiking duration in the lower trace (blue trace). Figure 5 shows the variation in the spiking duration with change in *Spiking Duration Control* voltage.

We tuned the axon hillock to different refractory periods and hence different firing frequencies by varying the control voltage *Refractory Period Control*. The action potentials generated by the test neuron (Neuron 1) were fed to the synapses of a similar second neuron (Neuron 2) and the output of Neuron 2 was observed. In Figure 3, when the output refractory period is adjusted to 30 ps (refractory period control=0.3 V) (red trace) then there is temporal summation on the synapses (purple trace) of Neuron 2 to further cause the dendritic voltage of Neuron 2 to temporally sum (blue trace). This

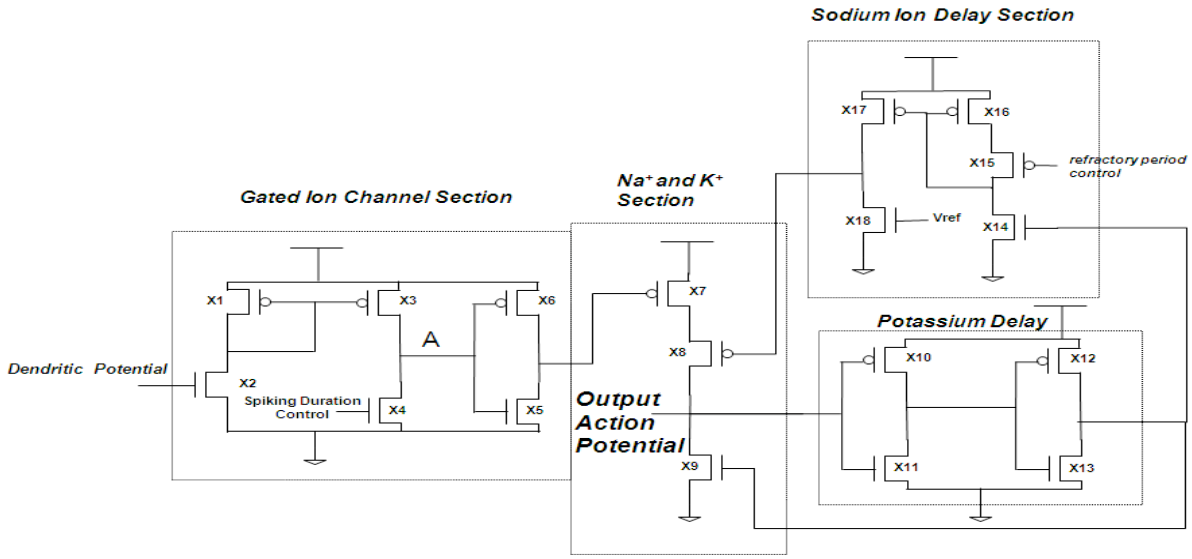

Fig. 1. The Axon Hillock Circuit

causes neuron 2 to produce an output train of action potentials (orange). On the other hand, as shown in Figure 4, when the output refractory period is adjusted to 50 ps (refractory period control=0.6 V) (red trace) there is no temporal summation on the synapses (purple trace) of Neuron 2 hence there is no temporal summation of the dendritic voltage (blue trace) which in turn fails to excite neuron 2 to produce a train of action potentials (orange trace at .048 mV).

V. Conclusion

A carbon nanotube cortical neuron with a tunable spiking axon hillock is presented here, and simulations testing the tunability are shown. Simulations have demonstrated changes in spiking frequency and spiking duration as control voltages are changed, resulting in biomimetic behavioral variations in spiking and post-synaptic neural stimulation.

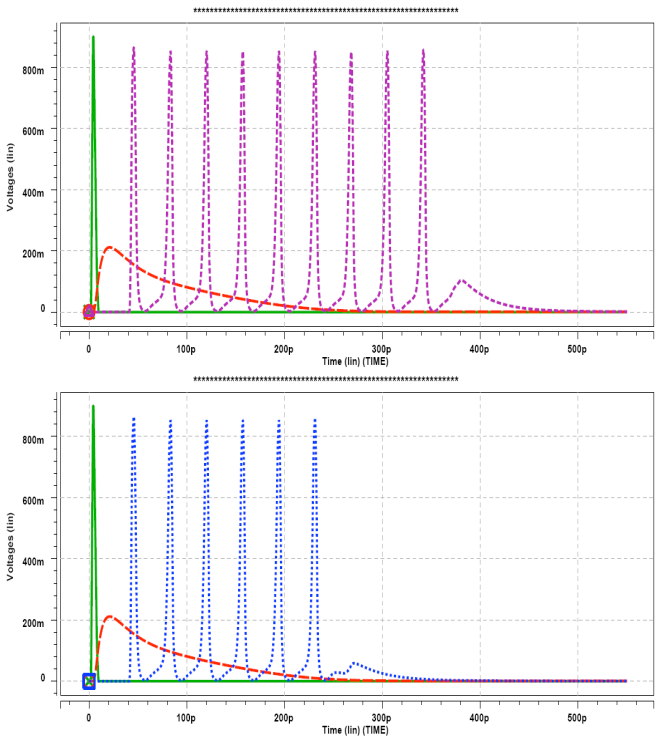

Fig. 2. Input action potential (green trace) and resultant increase in dendritic potential (red trace) leading to continuous neural spiking of higher duration (purple trace) and lower duration (blue trace)

References

[1] E. Kandel, J. Schwartz, and T. Jessel, *Principles of Neural Science*, vol. 4. McGraw-Hill, 2004.

[2] M. Beierlein, C. P. Fall, J. Rinzel, and R. Yuste, "Thalamocortical bursts trigger recurrent activity in neocortical networks: Layer 4 as a frequency-dependent gate," *J. Neurosci.*, vol. 22, pp. 9885–9894, November 2002.

[3] R. von der Heydt, H. Zhou, and H. S. Friedman, "Representation of stereoscopic edges in monkey visual cortex," *Vision Research*, vol. 40, pp. 1955–1967, July 2000.

[4] E. M. Izhikevich, "Simple model of spiking neurons," *Neural Networks, IEEE Transactions on*, vol. 14, no. 6, pp. 1569–1572, 2003.

[5] T. Tateno, A. Harsch, and H. P. C. Robinson, "Threshold firing frequency-current relationships of neurons in rat somatosensory cortex: Type 1 and type 2 dynamics," *J Neurophysiol*, vol. 92, pp. 2283–2294, October 2004.

[6] B. Liu and J. F. Frenzel, "A CMOS neuron for VLSI circuit implementation of pulsed neural networks," in *Industrial Electronics Society, IEEE 2002 28th Annual Conference of the*, vol. 4, pp. 3182–3185 vol.4, 2002.

[7] K. M. Hynna and K. Boahen, "Silicon neurons that burst when primed," in *Circuits and Systems, 2007. IEEE International Symposium on*, pp. 3363–3366, 2007.

[8] K. A. Zaghloul and K. Boahen, "Optic nerve signals in a neuromorphic chip ii: testing and results," *Biomedical Engineering, IEEE Transactions on*, vol. 51, no. 4, pp. 667–675, 2004.

[9] E. Farquhar and P. Hasler, "A bio-physically inspired silicon neuron," *Circuits and Systems I: Regular Papers, IEEE Transactions on*, vol. 52, no. 3, pp. 477–488, 2005.

[10] K. Nakada, T. Asai, and Y. Amemiya, "Analog CMOS implementation of a bursting oscillator with depressing synapse," in *Intelligent Sensors, Sensor Networks and Information Processing Conference, 2004. Proceedings of the 2004*, pp. 503–506, 2004.

[11] G. Indiveri, "A low-power adaptive integrate-and-fire neuron circuit,"

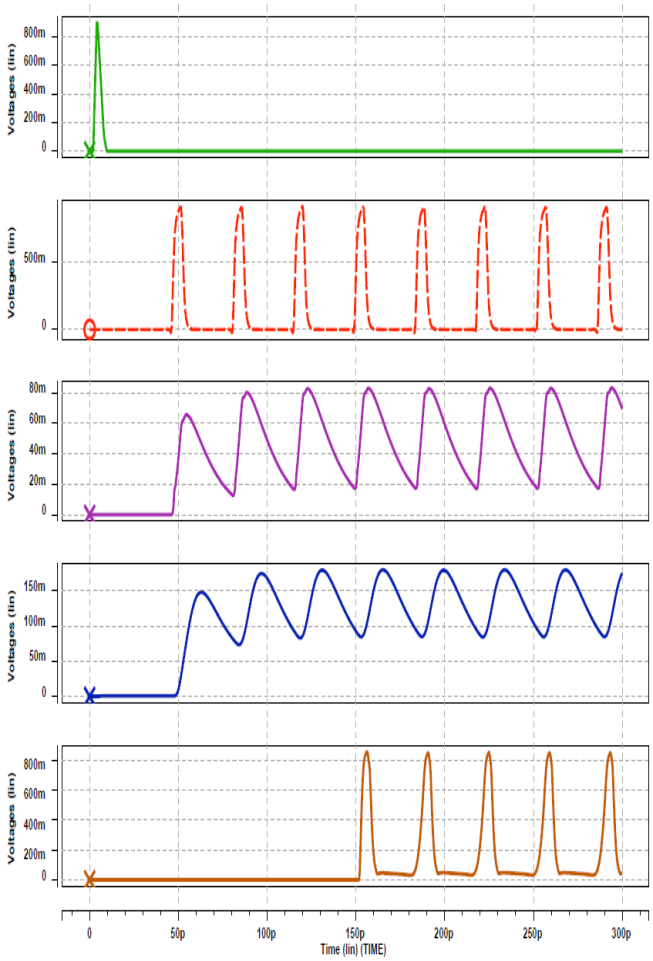

Fig. 3. High frequency firing in neuron 1 leads to an output spike train from neuron 2

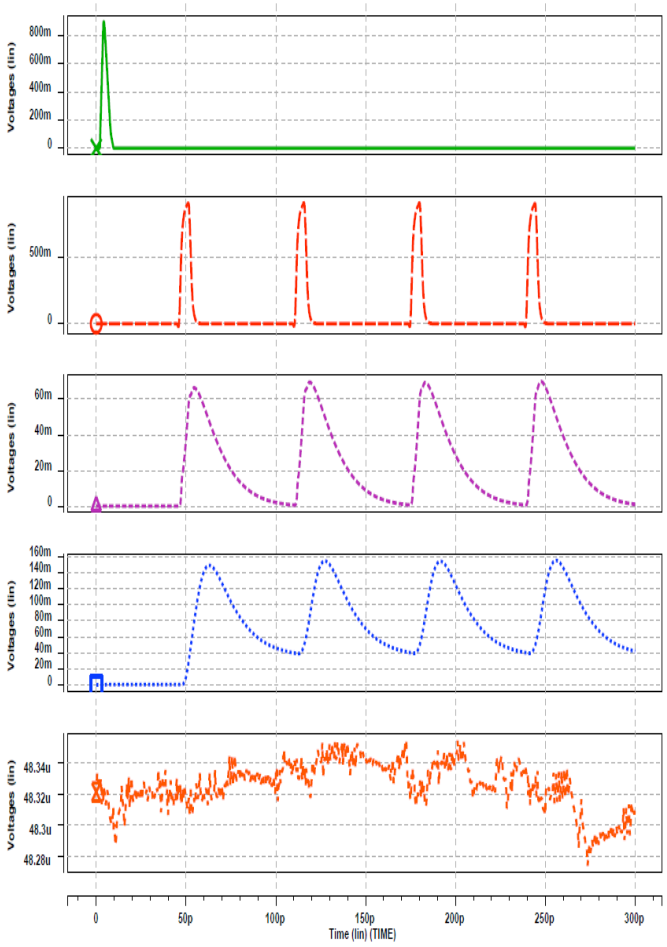

Fig. 4. Low frequency firing from Neuron 1 fails to produce an output from neuron 2

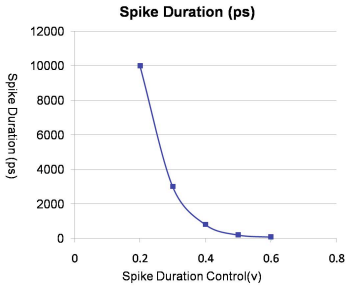

Fig. 5. Change in spike duration window with change in *Duration Control Voltage*

in *Circuits and Systems, 2003. Proceedings of the 2003 International Symposium on*, vol. 4, pp. IV–820–IV–823 vol.4, 2003.

[12] A. Bianco, R. Sainz, S. Li, H. Dumortier, L. Lacerda, K. Kostarelos, S. Giordani, and M. Prato, *Biomedical Applications of Functionalised Carbon Nanotubes*, pp. 23–50. 2008.

[13] A. C. Parker, A. Friesz, and K. Pakdaman, "Towards a nanoscale artificial cortex," in *Proceedings of The 2006 International Conference on Computing in Nanotechnology (CNAN'06)*, June 2006.

[14] B. C. Paul, S. Fujita, M. Okajima, T. H. Lee, H. S. P. Wong, and Y. Nishi, "Impact of a process variation on nanowire and nanotube device performance," *Electron Devices, IEEE Transactions on*, vol. 54, no. 9, pp. 2369–2376, 2007.

[15] N. Patil, J. Deng, A. Lin, H. S. P. Wong, and S. Mitra, "Design methods for misaligned and mispositioned carbon-nanotube immune circuits," *Computer-Aided Design of Integrated Circuits and Systems, IEEE Transactions on*, vol. 27, no. 10, pp. 1725–1736, 2008.

[16] X. Liu, S. Han, and C. Zhou, "Novel nanotube-on-insulator (noi) approach toward single-walled carbon nanotube devices," *Nano Letters*, vol. 6, pp. 34–39, January 2006.

[17] J. Deng and H. S. P. Wong, "A circuit-compatible spice model for enhancement mode carbon nanotube field effect transistors," in *Simulation of Semiconductor Processes and Devices, 2006 International Conference on*, pp. 166–169, 2006.

[18] J. Joshi, C. Hsu, A. Parker, and P. Deshmukh, "A carbon nanotube cortical neuron with excitatory and inhibitory dendritic computations," in *IEEE/NIH 2009 LIfe Science Systems and Applications Workshop*, 2009.

[19] A. K. Friesz and A. C. Parker, "A biomimetic carbon nanotube synapse," in *Biomedical Engineering Conference*, 2007.

[20] A. C. Parker, J. Joshi, C.-C. Hsu, and N. A. D. Singh, "A carbon nanotube implementation of temporal and spatial dendritic computations," in *Circuits and Systems, 2008. MWSCAS 2008. 51st Midwest Symposium on*, pp. 818–821, 2008.

[21] H. Chaoui, "CMOS analogue adder," *Electronics Letters*, vol. 31, no. 3, pp. 180–181, 1995.

[22] C. Yu-Ming, L. Rosene, J. Killiany, A. Mangiamele, and I. Luebke, "Increased action potential firing rates of layer 2/3 pyramidal cells in the prefrontal cortex are significantly related to cognitive performance in aged monkeys," *Cerebral Cortex*, vol. 15, pp. 409–418, April 2005.